Molecular Therapy
Oncolytics
Original Article

Knockdown of LRRN1 inhibits malignant phenotypes through the regulation of HIF-1α/Notch pathway in pancreatic ductal adenocarcinoma

Yalu Zhang,[1] Qiaofei Liu,[1] Sen Yang,[1] and Quan Liao[1]

[1]Department of General Surgery, State Key Laboratory of Complex Severe and Rare Diseases, Peking Union Medical College Hospital, Chinese Academy of Medical Science and Peking Union Medical College, Shuaifuyuan 1, Dongcheng District, Beijing 100730, China

Pancreatic ductal adenocarcinoma (PDAC) is one of the most refractory and fatal human malignancies. Leucine-rich repeat neuronal protein-1 (LRRN1) plays a crucial role in the development of the nervous system. However, the clinical implications and biological functions of LRRN1 in PDAC remain unclear. We found that LRRN1 expression was upregulated in PDAC tissues compared with paracancerous tissues and normal pancreatic tissues through the different public databases, tissue microarray-based immunohistochemistry, and dimethylbenzanthracene-induced PDAC murine model. The expression level of LRRN1 was closely related to the overall survival and disease-free survival of PDAC patients. Cox multivariate analysis indicated that LRRN1 was an independent adverse prognostic factor. The small hairpin RNA (shRNA)-mediated LRRN1 knockdown remarkably restrained the proliferative, migratory, and invasive capacities, as well as promoted cell apoptosis and increased G0/G1 arrest in PDAC cells. The xenograft murine subcutaneous bearing model and metastasis model verified that silencing of LRRN1 effectively dampened tumor growth and metastasis *in vivo*. Specifically, LRRN1 exerted its biological functions through the HIF-1α/Notch signaling pathway, and LRRN1 knockdown could dampen Jagged 1-mediated Notch pathway activation. Therefore, LRRN1 could serve as the potential therapeutic or prognostic target for PDAC.

INTRODUCTION

Pancreatic ductal adenocarcinoma (PDAC) is the most common pathological type of pancreatic cancer, accounting for around 90%.[1] It is well known that PDAC has lethal and refractory characteristics, including aggressive growth, distant metastatic potential, late-stage diagnosis, and resistance to adjuvant chemotherapy.[2] These factors result in a poor 5-year survival rate of only 9% in PDAC patients.[3] Although there are increasing studies on PDAC, the in-depth mechanisms concerning oncogenesis and tumor advancement remain to be illustrated. Therefore, it is of great significance to identify novel prognostic and therapeutic biomarkers by investigating the underlying pathological mechanisms of PDAC progression.

Leucine-rich repeat neuronal protein-1 (LRRN1, also known as NLRR1) was first discovered in the developing murine nervous system and played a pivotal role in neurodevelopmental and regenerative processes.[4–6] LRRN1 contributes to sustaining pluripotency and self-renewal potential of human embryonic stem cells through AKT phosphorylation to impede nuclear export of pluripotency-related protein, thus protecting them from post-translational degradation or modification.[7] Several recently published studies have suggested that LRRN1 exhibits an oncogenic function in neuroblastoma and gastric cancer (GC).[8,9] The biological roles and clinical implications of LRRN1 in PDAC are still unclear and remained to be illustrated.

The initiation and progression of PDAC is a multi-gene and multi-step process.[10–12] Among them, the hypoxic tumor microenvironment and the important signaling pathways are involved.[13] Hypoxia-inducible factor-1 alpha (HIF-1α) is a central regulator of cells in response to hypoxia in the microenvironment.[14] Under normoxia, HIF-1α can be degraded in a ubiquitin-proteasome fashion. In contrast, HIF-1α is stabilized under hypoxia by inhibiting its own hydroxylation and forms heterodimers with HIF-1β with the aid of coactivators, in turn transferring into nucleus to control the transcription of target genes.[15] Furthermore, hypoxia-activated HIF-1α has been reported to be involved in tumor metabolism and angiogenesis and to facilitate tumor metastasis and progression via activating the Notch pathway,[16] a critical regulatory signaling mechanism that governs cell fate determination and epithelial-mesenchymal transition (EMT) in PDAC.[17,18] Jagged 1 (JAG1) is a canonical ligand of the Notch signaling pathway in mammals.[19,20] As a Notch pathway-specific activator, JAG1 interacts with Notch receptor to activate the Notch pathway, incurring the shedding of Notch intracellular domain (NICD), and it binds with cofactors to stimulate substantial target gene expressions involved in various biological processes.[18,21,22] However, it is still unclear whether and how LRRN1 affects HIF-1α/Notch signaling in PDAC.

Received 12 June 2021; accepted 24 August 2021;
https://doi.org/10.1016/j.omto.2021.08.012.

Correspondence: Quan Liao, Department of General Surgery, State Key Laboratory of Complex Severe and Rare Diseases, Peking Union Medical College Hospital, Chinese Academy of Medical Science and Peking Union Medical College, Shuaifuyuan 1, Dongcheng District, Beijing 100730, China.
E-mail: liaoq@pumch.cn

This is an open access article under the CC BY-NC-ND license (http://creativecommons.org/licenses/by-nc-nd/4.0/).

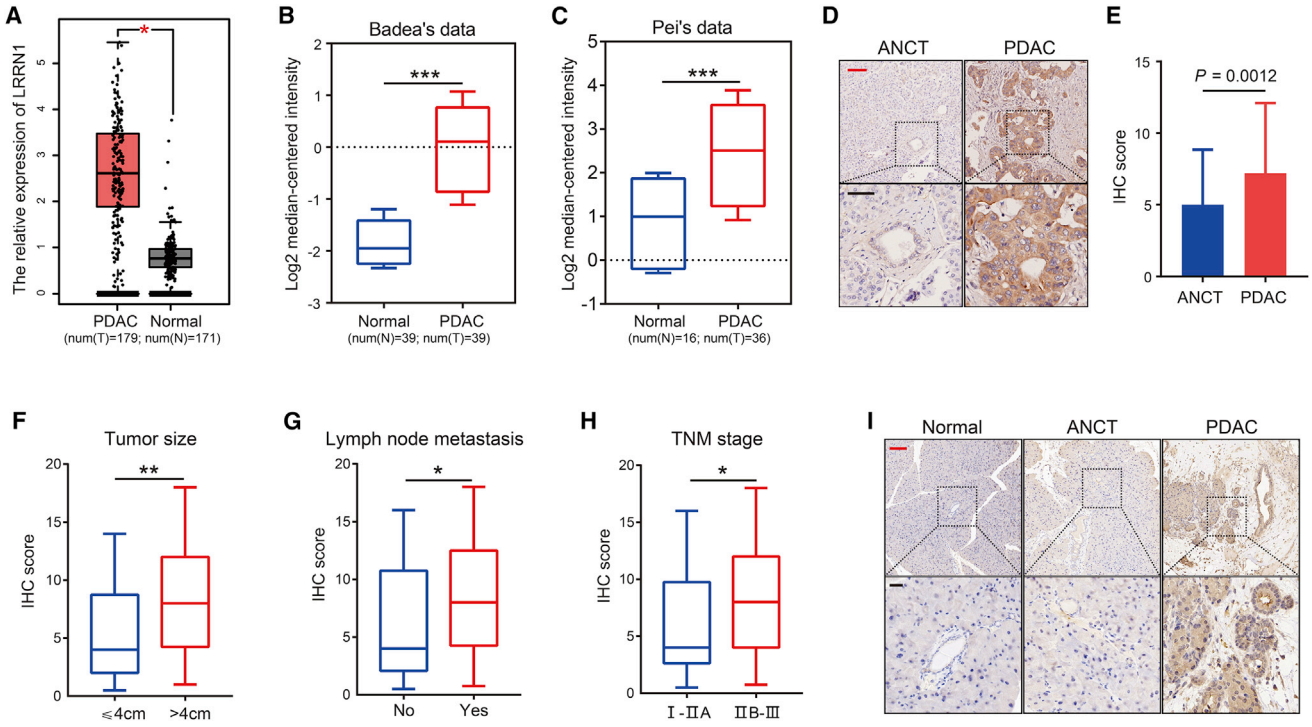

Figure 1. LRRN1 is highly expressed in PDAC tissues and associated with clinicopathologic characteristics

(A) In the GEPIA database, LRRN1 expression in PDAC tissues (n = 179) and normal pancreatic tissues (n = 171). (B and C) In the subsets of the Oncomine database, Badea and Pei's data exhibit the LRRN1 expression in normal pancreatic tissues and PDAC tissues (39 versus 39 and 16 versus 36, respectively). (D) The representative IHC staining for LRRN1. Red bar, 100 μm; black bar, 50 μm. ANCT, adjacent noncancerous tissue. (E) The IHC score of LRRN1 in 83 pairs of PDAC and ANCT. (F–H) The LRRN1 expression was higher in those with larger tumor size, positive lymph node metastasis, and advanced TNM stage. (I) The IHC of LRRN1 expression in normal pancreatic tissues, PDAC, and ANCT from DMBA-induced murine model. Red bar, 100 μm; black bar, 20 μm. *$p < 0.05$, **$p < 0.01$, ***$p < 0.001$.

Previously, we had screened LRRN1 by using the bioinformatics method, implying that it may be associated with the prognosis of PDAC patients, but no in-depth studies were investigated.[23] Herein, we examined LRRN1 expression and its prognosis correlation of PDAC patients based on the public databases, tissue microarray (TMA)-based immunohistochemistry (IHC), and dimethylbenzanthracene (DMBA)-induced PDAC murine model. Furthermore, a series of cellular function experiments and murine models were utilized to evaluate the roles of LRRN1 in proliferation, invasion, and migration of PDAC cells *in vitro* and *in vivo*. More importantly, we found that the biological role of LRRN1 was probably dependent on the HIF-1α/Notch signaling pathway, and knockdown of LRRN1 could dampen JAG1-mediated Notch signaling activation.

RESULTS

LRRN1 is highly expressed in PDAC tissues and related to clinicopathologic characteristics

To investigate LRRN1 expression in various tumor tissues, the different public databases were first explored. Using the GEPIA database, we analyzed LRRN1 expression across 33 types of cancer samples and corresponding normal tissues. The results displayed that the expression of LRRN1 was dramatically upregulated in PDAC tissues by comparing 179 PDAC tissues and 171 normal samples, in addition to aberrant expression in some neurological neoplasms (glioblastoma multiforme and brain low-grade gliomas) and reproductive neoplasms (prostate, uterine, testicular germ cell tumors) (Figure 1A; Figure S1A). The Oncomine database also showed that PDAC tissues expressed higher levels of LRRN1 than normal pancreatic tissues, apart from abnormal expression in nervous system neoplasms and leukemia (Figure S1B). Specifically, Badea and Pei's data indicated that LRRN1 expression was enhanced in PDAC tissues.[24,25] In order to verify these findings, we constructed a TMA-IHC containing 83 pairs of PDAC tissue and adjacent noncancerous tissue (ANCT). Our results confirmed the high expression of LRRN1 in PDAC tissues (Figures 1D and 1E). Furthermore, we also found that the LRRN1 expression was tightly correlated with tumor size, lymph node metastasis, and TNM stage, but it was unrelated to other clinical characteristics of patients with PDAC, including age, gender, tobacco use, alcohol use, histological grade, tumor location, perineural invasion, and macrovascular invasion (Figures 1F–1H; Table 1). More importantly, a murine model of DMBA-induced PDAC was established, and the IHC staining corroborated that LRRN1 expression was augmented in PDAC tissues compared with normal pancreatic tissues and ANCT (Figure 1I).

Table 1. Relationship between LRRN1 expression and clinicopathological characteristics of PDAC patients (n = 83)

		LRRN1 expression		
Parameters	Total	Low (n = 39)	High (n = 44)	p Value
Age (years)				
<60	40	18	22	0.726
≥60	43	21	22	
Gender				
Female	32	15	17	0.987
Male	51	24	27	
Tobacco use				
No	63	27	36	0.181
Yes	20	12	8	
Alcohol use				
No	68	31	37	0.586
Yes	15	8	7	
Histological grade				
G1–2	70	32	38	0.590
G3	13	7	6	
Tumor location				
Head	55	26	29	0.942
Body/tail	28	13	15	
Tumor size (cm)				
≤4	42	26	16	0.006*
>4	41	13	28	
Lymph node metastasis				
Negative	45	27	18	0.010*
Positive	38	12	26	
TNM stage				
I–IIA	40	24	16	0.022*
IIB–III	43	15	28	
Perineural invasion				
Negative	30	18	12	0.074
Positive	53	21	32	
Macrovascular invasion				
Negative	58	27	31	0.903
Positive	25	12	13	

*p < 0.05.

The upregulated LRRN1 is closely linked to poor prognosis of patients with PDAC

Next, we investigated the relationship between LRRN1 and the prognosis of PDAC patients. The LinkedOmics database demonstrated that PDAC patients with higher expression of LRRN1 had a worse clinical outcome (Figure 2A). The GEPIA database displayed that LRRN1 expression was negatively correlated with overall survival (OS) and disease-free survival (DFS) (Figures 2B and 2C). Similarly, the Kaplan-Meier plotter also demonstrated that LRRN1 expression was notably related to OS and relapse-free survival (RFS) in patients with PDAC (Figures 2D and 2E). The LRRN1 high-expression group had 1.62 times the risk of PDAC-related death versus the LRRN1 low-expression group, and the median OS time of the low- and high-expression groups were 24.6 months and 19.7 months, respectively (Figures 2D and 2E). The LRRN1 high-expression group had 3.41 times the risk of relapse in comparison to the LRRN1 low-expression group. The upper quartile RFS time of the low-expression group was 23.9 months, but that of the high-expression group was only 8.6 months (Figures 2D and 2E). Our cohort confirmed that the high expression of LRRN1 was an unfavorable factor for the prognosis of PDAC patients ($p = 0.0016$; Figure 2F). The median OS time of the low- and high-expression cohort was 17.4 months and 11.2 months, respectively (Figure 2F). These findings revealed that LRRN1 may be a powerful prognostic marker for patients with PDAC.

LRRN1 is an independent negative factor for PDAC patients

In addition to LRRN1, univariate analysis demonstrated that age, gender, tobacco use, tumor size, lymph node metastasis, TNM stage, and perineural invasion were relevant in prognosis of patients with PDAC (Table 2). We incorporated these indicators into a Cox proportional hazard model (Forward: LR). Multivariate analysis suggested that LRRN1 was an independent negative prognostic factor for patients with PDAC (Table 2). Moreover, the subgroup analysis of PDAC patients demonstrated that LRRN1 expression was an effective prognostic marker in groups with age less than 60 years ($p < 0.0001$), female ($p = 0.0056$), no tobacco use ($p = 0.0001$), no alcohol use ($p = 0.0001$), histological G1–2 ($p = 0.0036$), tumor location-body/tail ($p = 0.0005$), tumor size greater than 4 cm ($p = 0.0063$), lymph node metastasis-negative ($p = 0.0219$), TNM stage I–IIA ($p = 0.0473$), and perineural invasion-positive ($p = 0.0226$) (Table 3; Figure S2). With regard to macrovascular invasion, both the negative and positive subgroups were related to OS of patients with PDAC ($p = 0.0232$ and 0.0022, respectively) (Table 3; Figure S2).

Knockdown of LRRN1 inhibits the proliferation, facilitates cell apoptosis, and alters cell cycle in PDAC cells *in vitro*

To explore the roles of LRRN1 in PDAC cells, we detected the LRRN1 expression in multiple PDAC cell lines. Compared with human immortal pancreatic epithelial cell line HPNE, we observed that LRRN1 was highly expressed in most PDAC cell lines, except for Panc-1 (Figure 3A). We selected two cell lines with relatively high expression, AsPC-1 and BxPC-3, to silence the LRRN1 expression with small hairpin RNA (shRNA) for the following experiments. The successful stable knockdown of LRRN1 was verified at mRNA and protein levels (Figures 3B and 3C). The Cell Counting Kit-8 (CCK-8) and colony-formation assay revealed that LRRN1 silencing repressed the proliferation capacity and cell viability of PDAC (Figures 3D and 3E). Specifically, we further explored the apoptosis and cell cycle affecting cell proliferation. The flow cytometry analysis demonstrated that quiescence of LRRN1 resulted in an increased proportion of cell

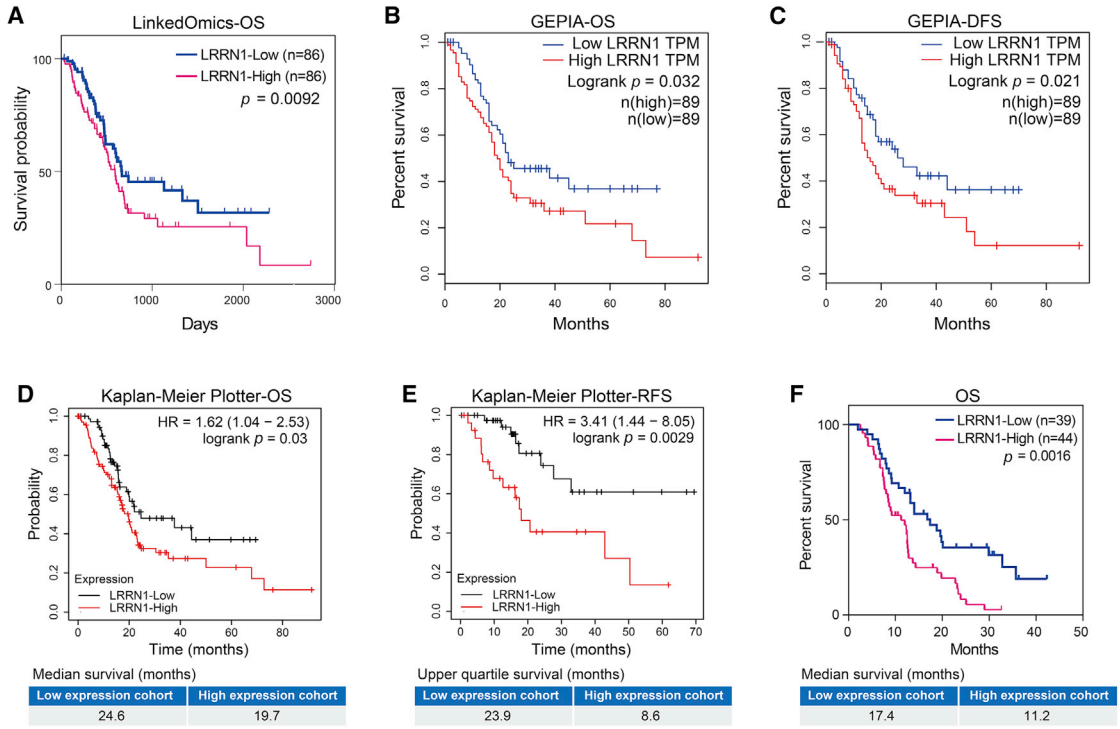

Figure 2. The upregulated LRRN1 is strongly correlated with the poor prognosis of patients with PDAC

(A and B) In the GEPIA database, the LRRN1 high-expression cohort (n = 89) had shorter OS and DFS than the LRRN1 low-expression cohort (n = 89) (p = 0.032 and 0.021, respectively). (C) In the LinkedOmics database, the LRRN1 expression is negatively linked to the OS of PDAC patients (86 versus 86, p = 0.0092). (D and E) The Kaplan-Meier plotter showed that LRRN1 was not only tightly related to the OS of patients (p = 0.03) but also a negative factor for RFS in PDAC (p = 0.0029). (F) Our data confirmed that PDAC patients with high LRRN1 expression had a worse clinical outcome than those with low LRRN1 expression (44 versus 39, p = 0.0016). OS, overall survival; DFS, disease-free survival; TPM, transcripts per million; RFS, relapse-free survival; HR, hazard ratio.

apoptosis, quiescent period G0/G1 arrest, and reduced proportion of division stage G2/M (Figures 3F and 3G). Furthermore, the apoptosis-associated and cell-cycle-associated proteins were evaluated by western blot. The results showed that anti-apoptosis factor Bcl-2 was downregulated, while pro-apoptosis protein Bax was upregulated, and the expression levels of cyclin D1 and CDK4 were diminished following LRRN1 knockdown (Figures 3H and 3I).

Silencing of LRRN1 inhibits the migration and invasion capacities of PDAC cells *in vitro*

We also detected the roles of LRRN1 in the migration and invasion of PDAC cells. The wound healing assays demonstrated that LRRN1 silencing reduced the migration rate of PDAC (Figure 4A). Transwell invasion assays indicated that LRRN1 knockdown diminished the number of invasive cells (Figure 4B). These results revealed that deficiency of LRRN1 could impair the migration and invasion capacities of PDAC cells. In addition, EMT-associated proteins were detected, and the data manifested that the level of E-cadherin was augmented, whereas the levels of N-cadherin and vimentin were reduced (Figures 4C and 4D), indicating LRRN1 knockdown could contribute to resisting the EMT process. Collectively, LRRN1 may play a crucial role in PDAC malignant phenotypes.

Silencing of LRRN1 suppresses malignant biological behaviors *in vivo*

To further clarify whether the knockdown of LRRN1 could inhibit tumor growth *in vivo*, AsPC-1 or BxPC-3 cell suspension was inoculated into the inguinal subcutis of immunodeficient nude mice, and tumor growth was monitored. We found that xenograft tumors of the sh-LRRN1 group had a lower volume and weight compared to that of the control group (Figures 5A–5F), implicating deficiency of LRRN1 effectively dampened tumor growth *in vivo*. The LRRN1 expression of the sh-LRRN1 group and sh-negative control (sh-NC) group were confirmed in xenograft tumors by using IHC and immunofluorescence (IF) (Figure 5G). We utilized TUNEL staining to evaluate apoptosis *in vivo* and found that the proportion of apoptosis in the sh-LRRN1 group was higher than that in the sh-NC group, thus confirming the findings of the *in vitro* experiment (Figure 5G). Additionally, murine tumor metastasis models were constructed by injecting the tail vein with AsPC-1 or BxPC-3 cell suspension. The results demonstrated that the LRRN1-knockdown group had fewer lung and liver metastases compared to the sh-NC group (Figures 6A–6D), suggesting that LRRN1 knockdown suppressed the distant metastasis of PDAC cells. EMT-related proteins were detected using IHC; the sh-LRRN1 group exhibited elevated E-cadherin and diminished N-cadherin and vimentin in

Table 2. Univariate and multivariate analyses for prognostic factors of PDAC

	Univariate analysis		Multivariate analysis	
Parameters	HR (95% CI)	p Value	HR (95% CI)	p Value
Age (years): ≥60 versus <60	1.796 (1.102–2.929)	0.019*	2.699 (1.581–4.606)	<0.001*
Gender: Male versus female	1.793 (1.059–3.036)	0.030*	–	–
Tabacco use: Yes versus no	1.828 (1.070–3.123)	0.027*	3.375 (1.850–6.156)	<0.001*
Alcohol use: Yes versus no	1.671 (0.937–2.980)	0.082	–	–
Histological grade: G1–2 versus G3	1.459 (0.779–2.733)	0.239	–	–
Tumor location: Head versus body/tail	1.233 (0.739–2.057)	0.422	–	–
Tumor size (cm) >4 versus ≤4	1.657 (1.013–2.712)	0.044*	2.434 (1.418–4.177)	0.001*
Lymph node metastasis: Positive versus negative	1.675 (1.030–2.725)	0.038*	1.733 (1.013–2.966)	0.045*
TNM stage: I–IIA versus IIB–III	1.798 (1.104–2.927)	0.018*	–	–
Perineural invasion: Positive versus negative	1.707 (1.011–2.884)	0.046*	–	–
Macrovascular invasion: Positive versus negative	1.470 (0.874–2.472)	0.146	–	–
LRRN1 expression: High versus low	2.220 (1.333–3.699)	0.002*	1.775 (1.025–3.073)	0.040*

HR, hazard ratio; CI, confidence interval.
*p < 0.05.

Table 3. The prognostic relevance of LRRN1 expression in PDAC subgroups in which the poorer overall survival of patients is significantly associated with high LRRN1 expression

Subgroups	HR	95% CI	p Value
Age < 60 years	2.392	1.120–5.110	<0.0001
Female	3.188	1.272–7.989	0.0056
Tobacco use, no	1.650	0.905–3.007	0.0001
Alcohol use, no	1.750	0.995–3.077	0.0001
Histological grade, G1–2	1.450	0.842–2.498	0.0036
Tumor location, body/tail	3.250	1.363–7.747	0.0005
Tumor size > 4 cm	1.989	0.932–4.244	0.0063
Lymph node metastasis, negative	1.647	0.849–3.169	0.0219
TNM stage, I–IIA	1.543	0.755–3.157	0.0473
Perineural invasion, positive	1.538	0.839–2.822	0.0226
Macrovascular invasion, negative	1.516	0.835–2.753	0.0232
Macrovascular invasion, positive	1.647	0.704–3.853	0.0022

HR, hazard ratio; CI, confidence interval.

distant metastases (Figure 6E). These *in vivo* data were consistent with our *in vitro* results.

LRRN1 exerts its biological functions through the HIF-1α/Notch signaling pathway

Given that LRRN1 expression was strongly correlated with tumor size in human specimens and tumor burden in the murine model, it was reasonable to speculate that LRRN1 might be closely related to the hypoxic PDAC microenvironment. As a key signaling pathway in response to low oxygen pressure, the Notch pathway was activated and potentiated in tumors to promote proliferation via controlling cell cycle and apoptosis and facilitate metastasis via regulating EMT progress, especially cadherin, to accelerate PDAC progression.[26,27] Therefore, we initially used public databases to investigate the expression correlation between LRRN1 and Notch pathway-related genes at the transcriptional level. The correlation analysis from GEPIA and TIMER databases showed that LRRN1 was profoundly linked to the expression of HIF-1α, Notch1, and downstream Hes1 in PDAC (Spearman correlation; Figures 7A and 7B), hinting LRRN1 may regulate the HIF-1α/Notch pathway, which exerts a crucial function in the initiation and progression of PDAC.[17,28]

Vascular-rich tissue located at the junction of tumor and adjacent normal tissue is regarded as the normoxic region, while the center of tumor tissue wrapped by fibrous tissue with insufficient blood supply is considered as the hypoxic region. Using IHC staining of the DMBA-induced PDAC murine model, we observed the interesting phenomenon that LRRN1 expression was higher in the hypoxic PDAC tissue than in the normoxic PDAC tissue (Figure 7C), indicating that LRRN1 may play a role in the regulation of hypoxia in PDAC. Furthermore, IF staining of xenograft murine subcutaneous bearing model revealed that HIF-1α expression was reduced after LRRN1 downregulation (Figure 7D). Then, we detected the expression of HIF-1α/Notch signaling-related protein by western blot; the results demonstrated that LRRN1 knockdown markedly reduced the expression of HIF-1α, Notch1, NICD, and Hes1 (Figure 7E). These findings confirmed our above-mentioned hypothesis.

We also designed the rescue experiments to evaluate the regulatory relationship between LRRN1 and Notch signaling pathway by using the specific agonist of the Notch signaling pathway, human recombinant JAG1. As a specific stimulator, recombinant JAG1 could effectively activate the Notch pathway (Figure 7F). The rescue experiments revealed that this effect could be significantly reversed by the knockdown of LRRN1 (Figure 7F), suggesting that LRRN1 silencing could abrogate the JAG1-mediated activation of the Notch signaling pathway. Taken together, our results revealed the underlying mechanism by which LRRN1 promotes PDAC growth and metastasis through the HIF-1α/Notch signaling pathway.

DISCUSSION

Herein, we found LRRN1 expression was highly expressed in PDAC tissues and negatively linked to prognosis of patients with PDAC based on different public databases, TMA-IHC we constructed, and a DMBA-induced PDAC murine model. Furthermore, knockdown

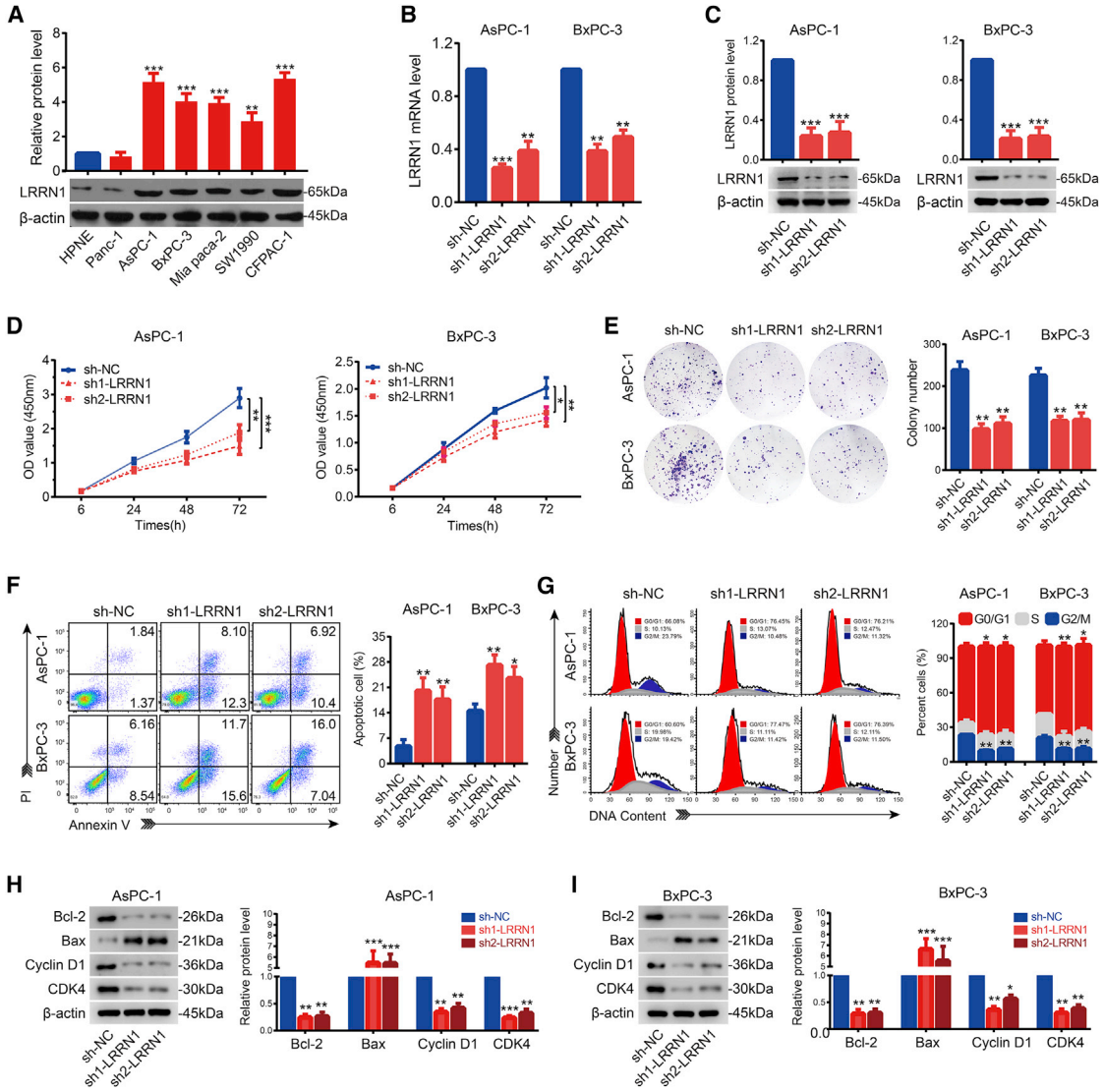

Figure 3. Knockdown of LRRN1 markedly inhibits proliferation, facilitates cell apoptosis, and alters the cell cycle in PDAC cells *in vitro*

(A) The LRRN1 expression in various PDAC cell lines and the human immortal pancreatic epithelial cell line HPNE. (B) AsPC-1 and BxPC-3 cells were infected with LRRN1-shRNA lentiviral particles (sh1-LRRN1 and sh2-LRRN1) and negative control (sh-NC). The expression level of LRRN1 mRNA was tested by PCR. (C) Transfection efficiency of LRRN1 shRNA was further verified by western blot. (D) CCK-8 assays showed that the optical density (OD) values of LRRN1-knockdown groups at 450 nm were notably lower than that of the NC group after 72 h. (E) Colony-formation assays revealed that cell viabilities were significantly reduced following the LRRN1 knockdown. (F) The shRNA-mediated LRRN1 silencing increased the cell apoptosis. (G) Flow cytometry displayed that LRRN1 knockdown fostered G0/G1 arrest and reduced the proportion of G2/M. (H and I) Deficiency of LRRN1 resulted in a reduction in the anti-apoptotic protein Bcl-2 and the cell cycle-related proteins cyclinD1 and CDK4, but an increase in the pro-apoptotic protein Bax. *p < 0.05, **p < 0.01, ***p < 0.001.

of LRRN1 markedly inhibited the proliferation, migration, and invasion capacities of PDAC cells *in vitro* and *in vivo*. More importantly, LRRN1 knockdown inhibited malignant biological behaviors of PDAC through abolishing HIF-1α/Notch pathway activation (Figure 7G).

It has been reported that LRRN1 expression in malignant neuroblastoma is higher than that in benign neuroblastoma, and upregulated LRRN1 often predicted an adverse clinical prognosis in patients with neuroblastoma.[29] Similarly, a recent study has revealed that LRRN1 was overexpressed in GC tissues, and high expression of LRRN1 was related to unfavorable clinical outcomes in GC patients.[9] Consistent with the above-mentioned findings, our data also showed that highly expressed LRRN1 was closely related to poor prognosis and was an independent negative prognostic factor of PDAC patients. LRRN1 expression has a good prognostic relevance with multiple

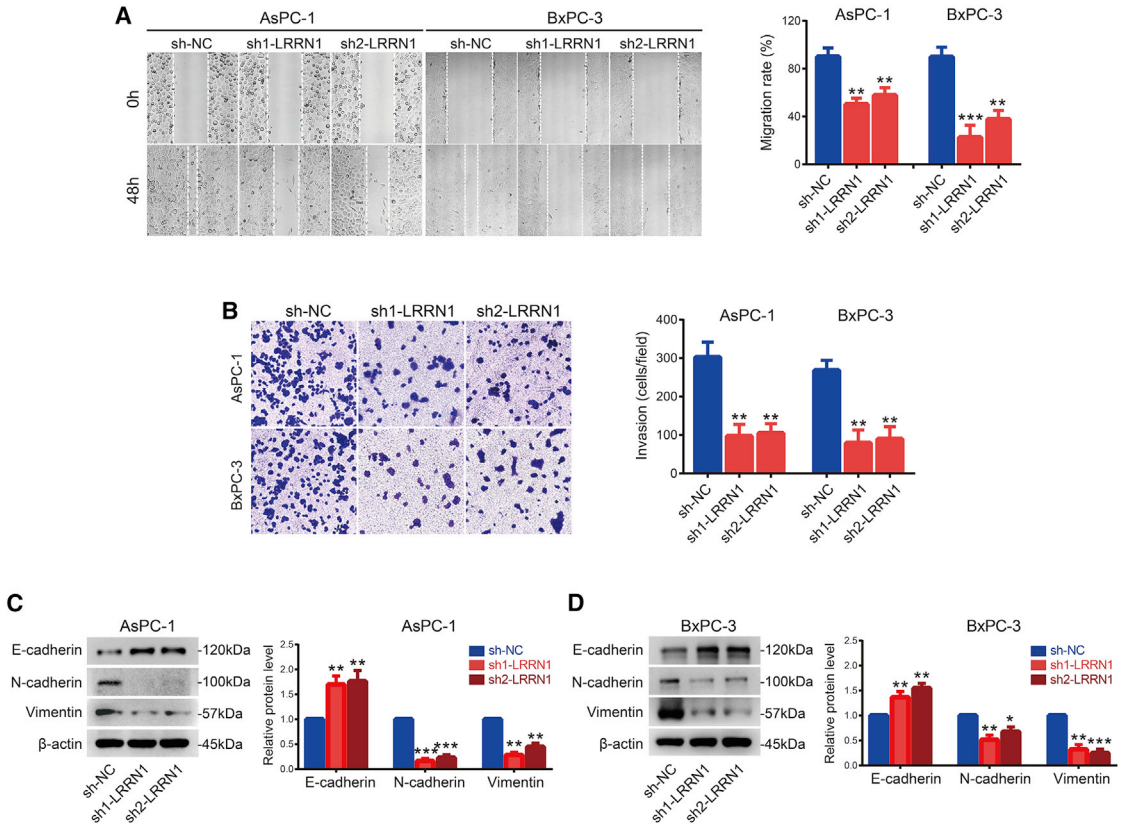

Figure 4. LRRN1 silencing notably represses the migration and invasion capacities of PDAC cells *in vitro*

(A) The wound-healing assays manifested that the LRRN1-knockdown groups had a lower migration rate than the sh-NC group. Magnification, 100×. (B) Transwell invasion assays demonstrated that the number of cell invasions was strikingly decreased in the LRRN1-knockdown groups compared with the sh-NC group. Magnification, 100×. (C and D) The silencing of LRRN1 led to an increase in E-cadherin and a reduction in N-cadherin and vimentin. *p < 0.05, **p < 0.01, ***p < 0.001.

PDAC subgroups. These results indicated that LRRN1 had an important value in predicting the prognosis and was likely to be an effective prognostic indicator for patients with PDAC. Furthermore, higher levels of LRRN1 were linked to older age and advanced stages in neuroblastoma.[29] In our study, LRRN1 expression was tightly relevant in tumor size, lymph node metastasis, and TNM stage in PDAC, but no correlations were found with age, gender, tobacco use, alcohol use, histological grade, tumor location, perineural invasion, and macrovascular invasion. Nevertheless, our cohort of PDAC paired specimens was limited concerning correlation analysis of LRRN1 expression and clinicopathological characteristics, which may result in statistical bias to some context. Therefore, it is necessary to further expand the sample size for investigation to obtain more reliable results.

In neuroblastoma, enhancement of LRRN1 expression protected neoplastic cells from serum starvation-induced apoptosis and facilitated cell proliferation through activating extracellular signal-related kinase mediated by IGF-1 and EGF.[30] In GC, LRRN1 inhibited tumor cell apoptosis through reducing the expression level of activator protein-1 (AP-1).[9] Our results provided evidence that the knockdown of LRRN1 boosted the cell apoptosis and increased G0/G1 arrest of the cell cycle, causing a reduction of proliferation in PDAC. Specifically, LRRN1 silencing elevated the level of Bax but diminished the level of Bcl-2. Bax and Bcl-2 are key modulators of the intrinsic pathway of apoptosis.[31,32] They can accumulate in the mitochondrial outer membrane to affect its permeabilization.[31] Bcl-2-mediated anti-apoptotic signals and Bax-mediated pro-apoptotic signals maintain the homeostasis of cell apoptosis.[32,33] However, alteration of LRRN1 expression broke the apoptotic balance sustained by Bcl-2/Bax, leading to increased cell apoptosis. We also found that cell-cycle-associated protein CDK4 and cyclin D1 were diminished following LRRN1 downregulation. Cyclin D1 and CDK4 are indispensable for the G1-to-S-phase transition by the formation of a complex to drive the cell cycle, ultimately resulting in the promotion of cell proliferation.[34] Taken together, altered expression levels of these proteins account for the reduced proliferation ability of PDAC cells following the LRRN1 knockdown.

Furthermore, LRRN1 silencing significantly dampened cell migration and invasion, in particular, accompanied by changes of EMT-related protein, that is, enhanced E-cadherin and curtailed N-cadherin and

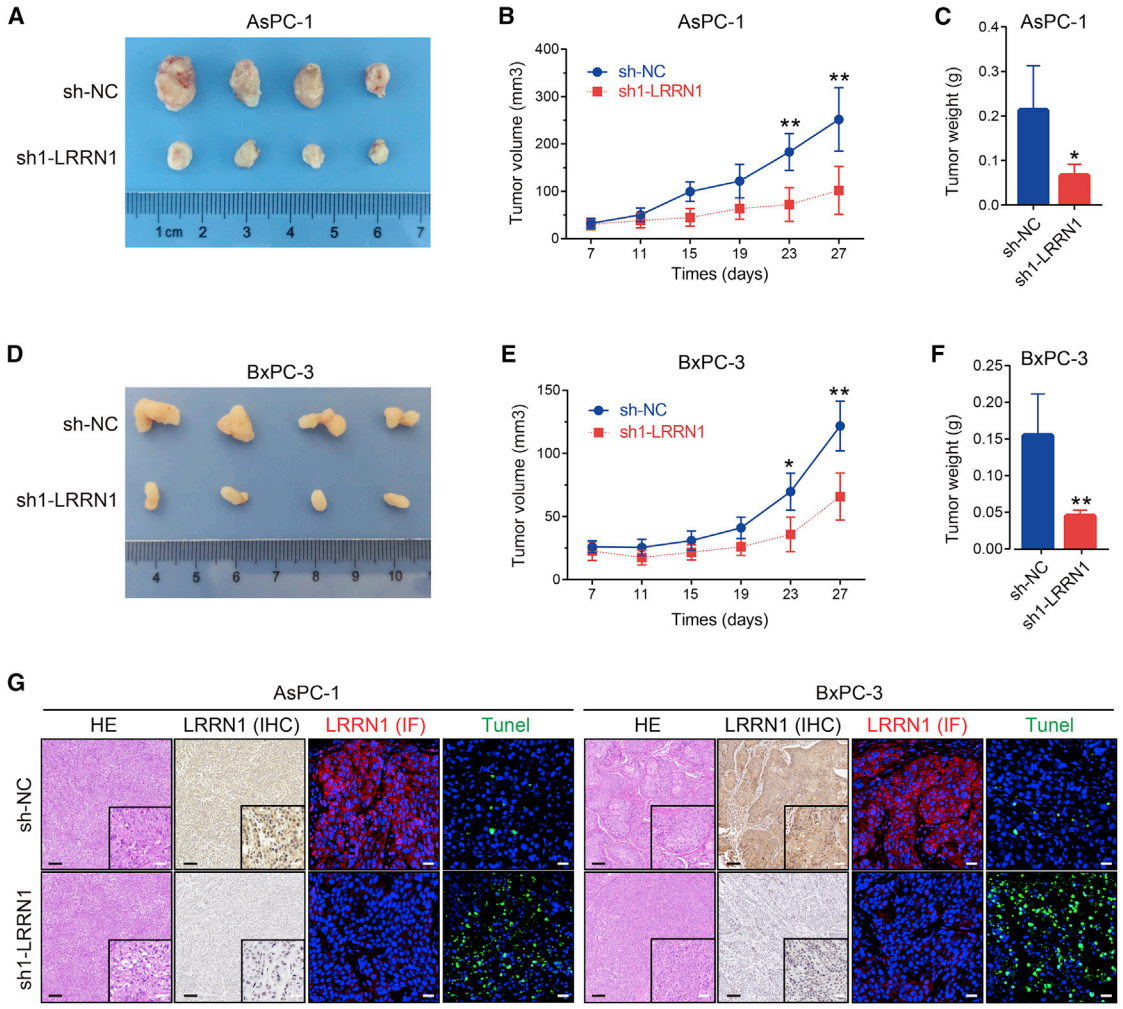

Figure 5. Silencing of LRRN1 significantly suppresses malignant biological behaviors *in vivo*

(A and D) AsPC-1 and BxPC-3 cells stably transfected with either sh-LRRN1 or sh-NC were subcutaneously inoculated into immunodeficient nude mice (n = 4 per group). (B and E) The volumetric growth curves of the tumor. The tumors were measured every 4 days from the second week. (C and F) The mice were euthanized, and subcutaneous tumors were weighed. (G) Representative images of IHC, IF, and TUNEL staining in tumor tissues. The IHC and IF confirmed that low expression of LRRN1 in tumor tissues stably transfected with LRRN1 shRNA. TUNEL staining was used to evaluate the proportion of apoptosis. LRRN1 (red), TUNEL (green), DAPI (blue). Black bar, 100 μm; white bar, 20 μm. NC, negative control; IHC, immunohistochemistry; IF, immunofluorescence. DAPI, 4′,6-diamidino-2-phenylindole. *$p < 0.05$, **$p < 0.01$.

vimentin. EMT is a crucial course of tumor cell metastasis, and it contains a series of physiological and pathological changes, in which decreased epithelial markers (E-cadherin) cause loss of intercellular adhesion, whereas enhanced mesenchymal markers (N-cadherin and vimentin) allow neoplastic cells to metastasize to distant tissues or organs.[35] Our data suggested that LRRN1 knockdown appears to be able to effectively resist this process, although the in-depth mechanism needs further investigation. More importantly, the murine xenograft model and tail vein tumor metastasis model confirmed these findings *in vitro*.

In GC, Liu et al.[9] observed that LRRN1 could resist cell apoptosis through inhibiting the Fas/FasL pathway. In contrast, we found that LRRN1 exerted its biological function through the HIF-1α/Notch signaling pathway. HIF-1α acts as a major transcriptional mediator in response to hypoxia response in the local PDAC tissue niche and controls substantial genes associated with hypoxic tension. Our data showed that knockdown of LRRN1 facilitated HIF-1α reduction and ameliorated HIF-1α-mediated hypoxic stress responses in the PDAC microenvironment, suggesting that LRRN1 might play a critical role in response to low oxygen tension of local PDAC tissue. Furthermore, activation of the Notch signaling pathway is often observed in the hypoxic tumor microenvironment.[16,36,37] Accumulating evidence confirms that Notch signaling activation contributes to the potentiation of aggressive properties, including cell proliferation, invasion, and angiogenesis within solid tumors.[22] The Notch pathway is reactivated during PDAC onset and progression.[17] One of the specific and effective ligands for Notch signaling activation is

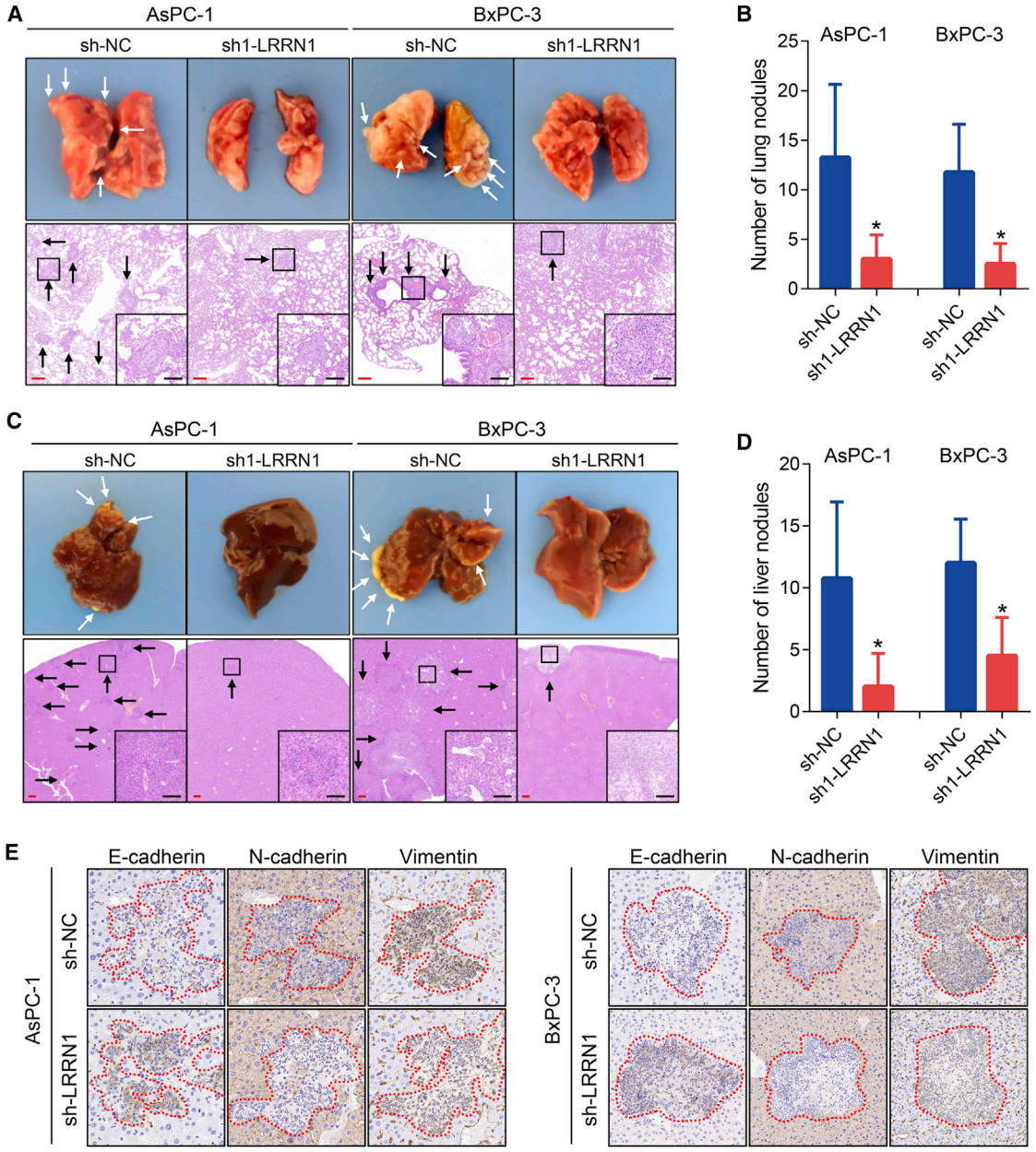

Figure 6. Silencing of LRRN1 effectively suppresses distant metastasis of PDAC *in vivo*

(A and C) The representative images of metastatic tumors in the lung and liver, as well as corresponding H&E staining of lung and liver tissues. Arrows indicate metastatic foci. Red bar, 200 μm; black bar, 100 μm. (B and D) The number of lung nodules and liver nodules from nude mice injected with AsPC-1 or BxPC-3 cells stably expressing sh-NC or sh-LRRN1. (E) The typical images of IHC for E-cadherin, N-cadherin, and vimentin in metastatic liver tissues. The *in vivo* model confirmed the results *in vitro* that silencing of LRRN1 enhanced the expression of E-cadherin while decreasing the expression of N-cadherin and vimentin. Magnification, 200×. *$p < 0.05$.

the JAG1, which has been reported to be highly expressed in PDAC tissues and tightly linked to shorter survival in PDAC patients.[38] The NICD can be released from the membrane in a proteolytic manner and is transported into the nucleus, where it complexes with CSL (CBF1/Su(H)/Lag-1), serving as an activator to stimulate a range of downstream gene expressions, such as Hes1 and CCND1.[21,22] Herein, we used recombinant JAG1 to activate the Notch signaling pathway successfully, while LRRN1 knockdown could inhibit the effect of JAG1-mediated Notch pathway activation, including the downstream NICD and Hes1, indicating LRRN1 may be a promising target for drug development. Of note, shRNA-mediated LRRN1 knockdown only partially rescued JAG1-mediated Notch signaling activation in AsPC-1 cells, whereas this effect was completely reversed in BxPC-3 cells. These findings suggested that

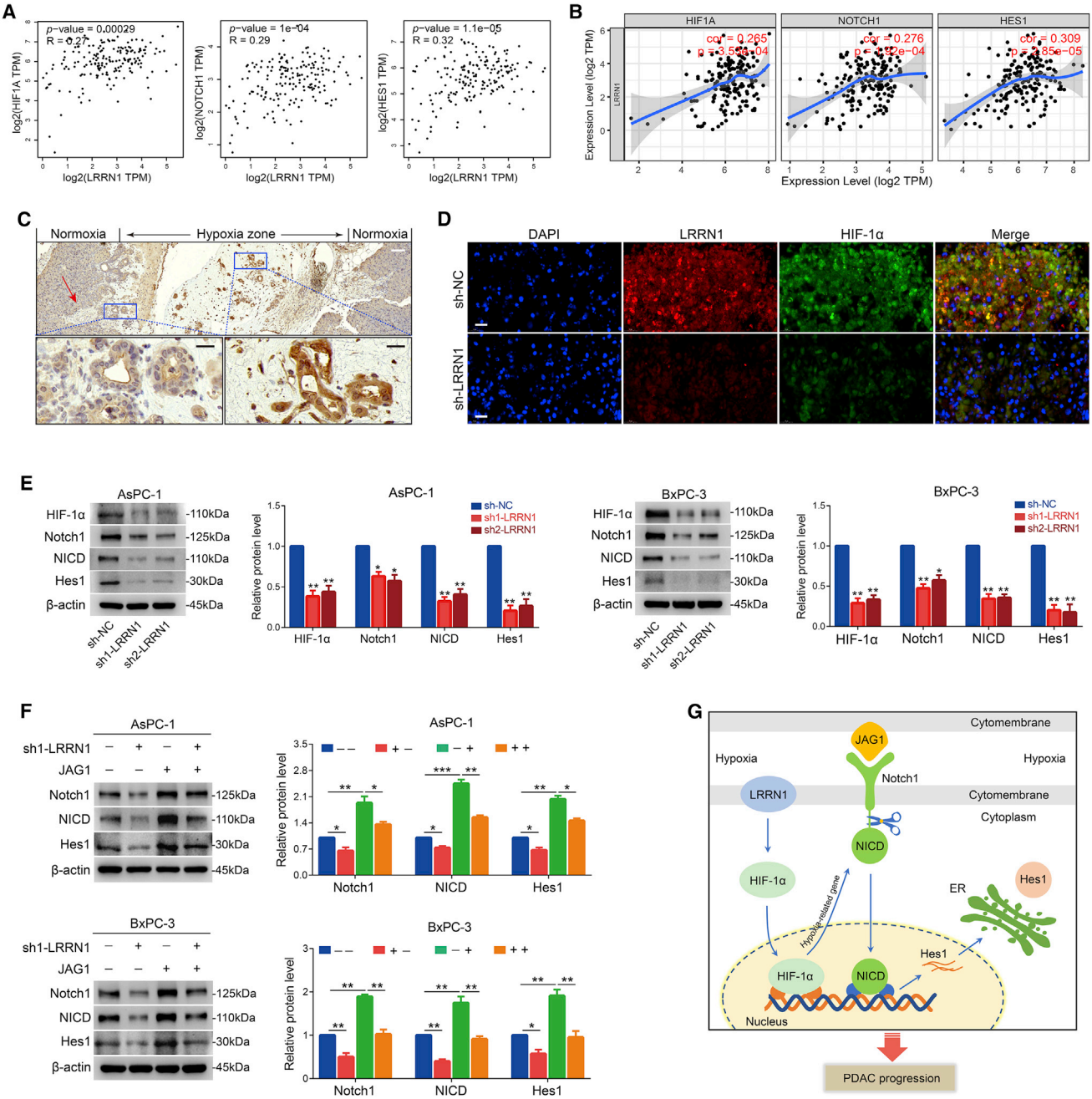

Figure 7. LRRN1 exerts its biological functions through the Notch signaling pathway

(A and B) GEPIA and TIMER databases were used to investigate the correlation between LRRN1 and HIF-1α, Notch1, as well as downstream Hes1 at the transcriptional levels (Spearman correlation). (C) IHC staining of PDAC tissues in different regions for LRRN1, including the junction of tumor tissue and adjacent normal tissue (normoxia zone) and the central area of fibrotic encapsulation (hypoxia zone). The red arrow points to the blood vessel. White bar, 100 μm; black bar, 20 μm. (D) IF staining of LRRN1 (red) and HIF-1α (green) in sh-LRRN1 group and control group by using xenograft murine subcutaneous bearing model (AsPC-1). White bar, 20 μm. (E) LRRN1 knockdown impaired the expression of HIF-1α/Notch pathway-related protein, including HIF-1α, Notch1, NICD, and Hes1. (F) The recombinant JAG1 stimulated the activation of Notch signaling, but this effect could be strongly dampened by the shRNA-mediated LRRN1 knockdown. (G) Schematic representation of LRRN1 promoting PDAC progression through the HIF-1α/Notch signaling pathway. *p < 0.05, **p < 0.01, ***p < 0.001.

BxPC-3 cells appear to be more sensitive to shRNA knockdown effects than AsPC-1 cells in the inhibition of JAG1-mediated Notch pathway activation.

In conclusion, the expression of LRRN1 is strongly upregulated in PDAC tissues and closely relevant in poor clinical outcomes of PDAC patients. Knockdown of LRRN1 effectively suppresses tumor growth and metastasis of PDAC *in vitro* and *in vivo*. LRRN1 exerts its biological functions through HIF-1α/Notch signaling, and its silencing can inhibit JAG1-mediated Notch pathway activation. Our results reveal a key oncogenic role for LRRN1 and could serve as a promising therapeutic or prognostic target for PDAC.

MATERIALS AND METHODS

Bioinformatics analysis

The LRRN1 expression in PDAC tissues and its correlation with prognosis of PDAC were investigated by the different online web tools, including GEPIA (http://gepia.cancer-pku.cn/),[39] Kaplan-Meier plotter (http://kmplot.com/analysis/),[40] LinkedOmics (http://www.linkedomics.orglogin.php),[41] and Oncomine (http://www.oncomine.org//).[42] In GEPIA, "Match TCGA normal and GTEx data" was selected for LRRN1 expression analysis, and "Median" was selected for survival analysis. In Oncomine, "Fold change > 2" and "p value < 1E−10" were selected as the screening conditions. The data of Badea and Pei belong to two subsets of them.

Patients and samples

A cohort of 83 patients with a pathological diagnosis of PDAC was enrolled between January 2008 and June 2011. PDAC tissues and paired paracancer tissues were screened and collected. A distance of more than 2 cm from the edge of lesion was defined as adjacent normal pancreatic tissue. Exclusion criteria adopted were as follows: (1) underwent preoperative radiotherapy or chemotherapy, (2) unable to obtain pathological specimens, (3) pathological diagnosis other than PDAC, (4) death in the perioperative period within 3 months, and (5) refused follow-up. The follow-up records and clinicopathological information were available for the enrolled patients. Diagnosis and staging of PDAC were based on the 7th edition of the American Joint Committee on Cancer (AJCC). The clinicopathological features of the enrolled patients with PDAC are summarized in Table 1. This study was approved by the Ethics Committee of Peking Union Medical College Hospital; all the patients enrolled provided written informed consent.

IF, H&E, and IHC Staining

The IF, hematoxylin and eosin (HE), and IHC staining were performed as described previously.[43–45] In brief, the tissue sections were fixed and stained with corresponding primary antibody (Table S1) and incubated with Alexa Fluor 546-labeled secondary antibody (Invitrogen, Waltham, MA, USA). Nuclei were treated with 4′,6-diamidino-2-phenylindole (DAPI). The sections were photographed with an inverted fluorescence microscope (Olympus, Japan). The One Step TUNEL Apoptosis Assay Kit was purchased from Beyotime Biotechnology (China, C1088) and performed according to protocols.

TMA construction and IHC evaluation

The PDAC-TMA (ZuoCheng Bio., China) was established to evaluate the expression of LRRN1 in pairs of PDAC tissue and ANCT through using formalin-fixed and paraffin-embedded blocks. After staining, TMA sections were digitalized by Panoramic MIDI scanning (3D Histech, Hungary). The staining evaluation was independently conducted by two investigators who were unable to obtain follow-up records of PDAC patients. For the same section with discordant scores, a consensus was reached after discussion. H-score based on staining proportion and intensity was adopted to assess the expression level of LRRN1.[44,46,47] According to the H-score median, the samples were classified into low- or high-LRRN1-expression groups.

Cell lines, transfection, and reagents

Human immortal pancreatic epithelial cell line HPNE and PDAC cell lines (Panc-1, AsPC-1, BxPC-3, Mia Paca-2, SW1990, CAPAC-1) were cultured in DMEM or RPMI-1640 medium (HyClone, Thermo Fisher, Waltham, MA, USA) containing 10% fetal bovine serum (FBS) (Gibco, Waltham, MA, USA) and 1% penicillin-streptomycin (Sigma, St. Louis, MO, USA) at 5% CO_2 and 37°C. The transfection of PDAC cells was performed using Lipofectamine 3000 Reagent (Invitrogen, Waltham, MA, USA) in accordance with the manual. The shRNA and NC were synthesized and purchased by GeneChem (Shanghai, China). The target sequence of LRRN1 shRNA was as follows: sh1-LRRN1: 5′-CCACTCATTAACCTCTGGGAA-3′; sh2-LRRN1: 5′-CCACCTGAACTCCAACAAATT-3′. PDAC cells were infected with lentiviral vector carrying sh1-LRRN1, sh2-LRRN1, or NC for 48–72 h. Stable clones were screened for 2 weeks in the presence of puromycin. The efficiency of LRRN1 knockdown was verified at mRNA and protein levels using PCR and western blot, respectively. Human recombinant JAG1 protein (ab108575, Abcam, UK) was used to activate the Notch pathway.

Real-time qPCR

The extraction of total RNA from AsPC-1 and BxPC-3 cells was performed using Trizol Reagent (cat. no. 9108, Takara). The RNA was reverse-transcribed into cDNA using PrimeScript RT reagent Kit (cat. no. RR037A, Takara). Real-time quantitative PCR was administrated by TB Green Premix Ex Taq (cat. no. RR420A, Takara) on the QuantStudio3 (Applied Biosystems). All samples were analyzed in triplicate, and GAPDH was a standard endogenous control. The data were analyzed using the $2^{-\Delta\Delta CT}$ method. The primer sequences in the present study were as follows: LRRN1-F, 5'-GATAGCCT TGAGAGCCTGTC-3'; LRRN1-R, 5'-AGTCCCCTTCTTGGATT TTG-3'; GAPDH-F, 5'-CATGAGAAGTATGACAACAGCCT-3'; GAPDH-R, 5'-AGTCCTTCCACGATACCAAAGT-3'.

Western blot

The total cell lysates were harvested using a 2% SDS lysis buffer on ice. After the determination of protein concentration, the protein samples were loaded into wells for electrophoresis through 8% or 12% SDS-PAGE gels. The protein bands were separated and transferred into a nitrocellulose membrane (Millipore, Ireland). Then, the membrane

was blocked in 5% fat-free milk for 60 min and incubated overnight at 4°C with the primary antibodies (Table S2). The next day, the membranes were washed three times with Tris-buffered saline and Tween 20 (TBST) and then incubated for 60 min in horseradish peroxidase (HRP)-labeled secondary antibody (1:5,000, Zsbio, Beijing, China). The bands were visualized using an enhanced chemiluminescence (ECL) Kit (Applygen, China) in a Tanon 5200 Multi-imaging system (Tanon, China).

Cell-proliferation and colony-formation assays

The proliferative capacities of PDAC cells were detected using CCK-8 (Dojindo) in accordance with the protocols. Briefly, PDAC cells were seeded into a 96-well plate and absorbance was evaluated at 450 nm for 6, 24, 48, and 72 h using a microplate reader. Regarding colony-formation assay, the equal PDAC cells were seeded in six-well plates and cultured in complete medium. After 14 days, the colonies were stained with 0.1% crystal violet (Sangon Biotech, China). The visible colonies of each well were photographed and counted.

Flow cytometry

The AsPC-1 and BxPC-3 cells were collected and pretreated with 70% ethanol for 1 h on ice. Afterward, the cells were washed by PBS and incubated with appropriate RNase for 30 min at 37°C. For cell cycle, the cells were labeled using propidium iodide (PI), and the cycle distribution of PDAC cells was analyzed by a flow cytometer. For cell apoptosis, PDAC cells were dual stained using PI and Annexin-V-fluorescein isothiocyanate (FITC) in the dark, and then the percentages of cell apoptosis were determined by the FACSCanto II (BD Biosciences). Each sample was conducted in triplicate and repeated three times.

Wound-healing assays

PDAC cell suspension was added into 6-well plates and incubated up to 80%–90% confluence. A sterile pipette tip (200 μL) was utilized to scratch the center of each well along with a straight ruler. Photographs were taken at the time of scratch formation and 48 h later, respectively. The scratches need to be gently washed with PBS to remove the exfoliated cell debris prior to photographing. The cell migration rates were calculated using ImageJ software.

Transwell invasion assays

Cell invasion capacity was evaluated using Transwell chambers (8 μm pore, Corning, Corning, NY, USA) with Matrigel (BD Biosciences). A total of 1×10^5 cells (AsPC-1 and BxPC-3) with 100 μL serum-free medium were added into the upper chamber, while the 500 μL culture medium with 20% FBS was added into the lower chamber. After incubation for 48 h, the non-invading cells were removed with a swab. The invading cells were fixed and stained with 0.1% crystal violet (Sangon Biotech) for 20 min and washed three times with PBS. The invasive cells were photographed and counted in five random fields per well using a microscope.

DMBA-induced PDAC murine model

The male 5- or 6-week-old C57BL/6J mice were obtained from the Vital River Animal Center (Beijing, China). The spontaneous PDAC model was established as described previously.[45] Briefly, after fasting for 6 h, an incision of about 1 cm was made along the midline of the mouse's abdomen under anesthesia. The distal pancreas was softly pulled out from the posterior abdomen and an appropriate amount of DMBA crystal, a strong carcinogen, was carefully embedded into the distal pancreas. After ensuring that the DMBA did not overflow, a purse-string suture was performed, and the abdominal cavity was closed. Mice were monitored daily. Approximately 2 months after surgery, the mice were euthanized under anesthesia and pancreatic lesions were analyzed.

Nude mice xenograft studies

The male 5- or 6-week-old BALB/c nude mice were raised under specific pathogen-free conditions. All mice were randomly separated into eight groups of four mice each. For the xenograft model, PDAC cells stably transfected with sh-NC or sh-LRRN1 (100 μL PBS with 10^7 cells per mouse) were inoculated subcutaneously into the groin of mice. Tumor volume was monitored starting in the second week after inoculation, and subcutaneous tumors were measured every 4 days. The calculation formula of tumor volume (V) was as follows: $V = (\text{length}) \times (\text{width})^2 \times 0.5$. Finally, the nude mice were euthanized, and tumor samples were harvested and weighed. For the tail vein tumor metastasis model, PDAC cells (100 μL PBS with 5×10^6 cells per mouse) expressing with sh-NC or sh-LRRN1 were injected into the tail vein of mice. After 28 days, the nude mice were euthanized, and lung and liver tissues were collected. All animal experiments were approved by the Animal Ethics Committee of Peking Union Medical College Hospital.

Statistical analysis

Statistical analysis was conducted by SPSS Statistics 21.0 (Chicago, IL, USA), and graphs were plotted by GraphPad Prism 6.0 (La Jolla, CA, USA). The comparison of LRRN1 expression between cancer and paracancer tissues was evaluated using paired Wilcoxon test. The correlations between LRRN1 and clinicopathologic features were assessed by the Pearson chi-square test. The Kaplan-Meier method and log-rank test were employed to analyze the survival of PDAC patients. The multivariable analysis was conducted by the Cox proportional hazards model (Forward: LR). According to distributed data, the Mann-Whitney *U* test or Student's t test was used to compare the difference between the two groups. Among multiple groups, the one-way ANOVA with post hoc Dunnett test or Tukey's test was employed for the comparison. A two-tailed p value < 0.05 was regarded as statistically significant.

SUPPLEMENTAL INFORMATION

Supplemental information can be found online at https://doi.org/10.1016/j.omto.2021.08.012.

ACKNOWLEDGMENTS

This work was supported by the National Natural Science Foundation of China (81872501, 81673023, 81272573, and 81502068), the Beijing

Natural Science Foundation (7172177), and the Youth Foundation of Peking Union Medical College Hospital (pumch201911866). We would like to acknowledge Dr. Yunfeng Zhang and Yinuo Zhang for their valuable encouragement and spiritual support.

AUTHOR CONTRIBUTIONS

Y.Z. designed and performed related experiments and wrote the original draft; Q. Liu analyzed data and revised the manuscript; S.Y. participated in animal experiments and revised the manuscript; Q. Liao administrated and supervised the whole project. All authors read and approved the final manuscript.

DECLARATION OF INTERESTS

The authors declare no competing interests.

REFERENCES

1. Kamisawa, T., Wood, L.D., Itoi, T., and Takaori, K. (2016). Pancreatic cancer. Lancet *388*, 73–85.
2. Leonhardt, C.S., Traub, B., Hackert, T., Klaiber, U., Strobel, O., Büchler, M.W., and Neoptolemos, J.P. (2020). Adjuvant and neoadjuvant chemotherapy in pancreatic ductal adenocarcinoma. J. Pancreatol. *3*, 1–11.
3. Hussain, S.P. (2016). Pancreatic Cancer: Current Progress and Future Challenges. Int. J. Biol. Sci. *12*, 270–272.
4. Taguchi, A., Wanaka, A., Mori, T., Matsumoto, K., Imai, Y., Tagaki, T., and Tohyama, M. (1996). Molecular cloning of novel leucine-rich repeat proteins and their expression in the developing mouse nervous system. Brain Res. Mol. Brain Res. *35*, 31–40.
5. Andreae, L.C., Peukert, D., Lumsden, A., and Gilthorpe, J.D. (2007). Analysis of Lrrn1 expression and its relationship to neuromeric boundaries during chick neural development. Neural Dev. *2*, 22.
6. Buchser, W.J., Slepak, T.I., Gutierrez-Arenas, O., Bixby, J.L., and Lemmon, V.P. (2010). Kinase/phosphatase overexpression reveals pathways regulating hippocampal neuron morphology. Mol. Syst. Biol. *6*, 391.
7. Liao, C.H., Wang, Y.H., Chang, W.W., Yang, B.C., Wu, T.J., Liu, W.L., Yu, A.L., and Yu, J. (2018). Leucine-Rich Repeat Neuronal Protein 1 Regulates Differentiation of Embryonic Stem Cells by Post-Translational Modifications of Pluripotency Factors. Stem Cells *36*, 1514–1524.
8. Hossain, S., Takatori, A., Nakamura, Y., Suenaga, Y., Kamijo, T., and Nakagawara, A. (2012). NLRR1 enhances EGF-mediated MYCN induction in neuroblastoma and accelerates tumor growth in vivo. Cancer Res. *72*, 4587–4596.
9. Liu, B., Zhang, Y., Fan, Y., Wang, S., Li, Z., Deng, M., Li, C., Wang, J., Ma, R., Wang, X., et al. (2019). Leucine-rich repeat neuronal protein-1 suppresses apoptosis of gastric cancer cells through regulation of Fas/FasL. Cancer Sci. *110*, 2145–2155.
10. Zhang, Y., Liu, Q., and Liao, Q. (2020). CircHIPK3: a promising cancer-related circular RNA. Am. J. Transl. Res. *12*, 6694–6704.
11. Zhang, Y., Liu, Q., and Liao, Q. (2020). Long noncoding RNA: a dazzling dancer in tumor immune microenvironment. J. Exp. Clin. Cancer Res. *39*, 231.
12. Neoptolemos, J.P., Kleeff, J., Michl, P., Costello, E., Greenhalf, W., and Palmer, D.H. (2018). Therapeutic developments in pancreatic cancer: current and future perspectives. Nat. Rev. Gastroenterol. Hepatol. *15*, 333–348.
13. Laitala, A., and Erler, J.T. (2018). Hypoxic Signalling in Tumour Stroma. Front. Oncol. *8*, 189.
14. Jin, X., Dai, L., Ma, Y., Wang, J., and Liu, Z. (2020). Implications of HIF-1α in the tumorigenesis and progression of pancreatic cancer. Cancer Cell Int. *20*, 273.
15. Freedman, S.J., Sun, Z.Y., Poy, F., Kung, A.L., Livingston, D.M., Wagner, G., and Eck, M.J. (2002). Structural basis for recruitment of CBP/p300 by hypoxia-inducible factor-1 alpha. Proc. Natl. Acad. Sci. USA *99*, 5367–5372.
16. Landor, S.K., and Lendahl, U. (2017). The interplay between the cellular hypoxic response and Notch signaling. Exp. Cell Res. *356*, 146–151.
17. Avila, J.L., and Kissil, J.L. (2013). Notch signaling in pancreatic cancer: oncogene or tumor suppressor? Trends Mol. Med. *19*, 320–327.
18. Akil, A., Gutiérrez-García, A.K., Guenter, R., Rose, J.B., Beck, A.W., Chen, H., and Ren, B. (2021). Notch Signaling in Vascular Endothelial Cells, Angiogenesis, and Tumor Progression: An Update and Prospective. Front. Cell Dev. Biol. *9*, 642352.
19. Lai, E.C. (2004). Notch signaling: control of cell communication and cell fate. Development *131*, 965–973.
20. Li, D., Masiero, M., Banham, A.H., and Harris, A.L. (2014). The notch ligand JAGGED1 as a target for anti-tumor therapy. Front. Oncol. *4*, 254.
21. Kopan, R., and Ilagan, M.X. (2009). The canonical Notch signaling pathway: unfolding the activation mechanism. Cell *137*, 216–233.
22. Misiorek, J.O., Przybyszewska-Podstawka, A., Kałafut, J., Paziewska, B., Rolle, K., Rivero-Müller, A., and Nees, M. (2021). Context Matters: NOTCH Signatures and Pathway in Cancer Progression and Metastasis. Cells *10*, 94.
23. Zhang, Y., Zhang, R., Ding, X., and Ai, K. (2018). EFNB2 acts as the target of miR-557 to facilitate cell proliferation, migration and invasion in pancreatic ductal adenocarcinoma by bioinformatics analysis and verification. Am. J. Transl. Res. *10*, 3514–3528.
24. Badea, L., Herlea, V., Dima, S.O., Dumitrascu, T., and Popescu, I. (2008). Combined gene expression analysis of whole-tissue and microdissected pancreatic ductal adenocarcinoma identifies genes specifically overexpressed in tumor epithelia. Hepatogastroenterology *55*, 2016–2027.
25. Pei, H., Li, L., Fridley, B.L., Jenkins, G.D., Kalari, K.R., Lingle, W., et al. (2009). FKBP51 affects cancer cell response to chemotherapy by negatively regulating Akt. Cancer Cell *16*, 259–266.
26. Gao, J., Long, B., and Wang, Z. (2017). Role of Notch signaling pathway in pancreatic cancer. Am. J. Cancer Res. *7*, 173–186.
27. Li, X.Y., Zhai, W.J., and Teng, C.B. (2015). Notch Signaling in Pancreatic Development. Int. J. Mol. Sci. *17*, 48.
28. Timmerman, L.A., Grego-Bessa, J., Raya, A., Bertrán, E., Pérez-Pomares, J.M., Díez, J., Aranda, S., Palomo, S., McCormick, F., Izpisúa-Belmonte, J.C., and de la Pompa, J.L. (2004). Notch promotes epithelial-mesenchymal transition during cardiac development and oncogenic transformation. Genes Dev. *18*, 99–115.
29. Hamano, S., Ohira, M., Isogai, E., Nakada, K., and Nakagawara, A. (2004). Identification of novel human neuronal leucine-rich repeat (hNLRR) family genes and inverse association of expression of Nbla10449/hNLRR-1 and Nbla10677/hNLRR-3 with the prognosis of primary neuroblastomas. Int. J. Oncol. *24*, 1457–1466.
30. Hossain, M.S., Ozaki, T., Wang, H., Nakagawa, A., Takenobu, H., Ohira, M., Kamijo, T., and Nakagawara, A. (2008). N-MYC promotes cell proliferation through a direct transactivation of neuronal leucine-rich repeat protein-1 (NLRR1) gene in neuroblastoma. Oncogene *27*, 6075–6082.
31. Peña-Blanco, A., and García-Sáez, A.J. (2018). Bax, Bak and beyond - mitochondrial performance in apoptosis. FEBS J. *285*, 416–431.
32. Zhang, Y., Zhang, R., Luo, G., and Ai, K. (2018). Long noncoding RNA SNHG1 promotes cell proliferation through PI3K/AKT signaling pathway in pancreatic ductal adenocarcinoma. J. Cancer *9*, 2713–2722.
33. Zheng, J.H., Viacava Follis, A., Kriwacki, R.W., and Moldoveanu, T. (2016). Discoveries and controversies in BCL-2 protein-mediated apoptosis. FEBS J. *283*, 2690–2700.
34. Tchakarska, G., and Sola, B. (2020). The double dealing of cyclin D1. Cell Cycle *19*, 163–178.
35. Träger, M.M., and Dhayat, S.A. (2017). Epigenetics of epithelial-to-mesenchymal transition in pancreatic carcinoma. Int. J. Cancer *141*, 24–32.
36. De Francesco, E.M., Maggiolini, M., and Musti, A.M. (2018). Crosstalk between Notch, HIF-1α and GPER in Breast Cancer EMT. Int. J. Mol. Sci. *19*, 2011.
37. Mu, R., Zou, Y.K., Tu, K., Wang, D.B., Tang, D., Yu, Z., and Zhao, L. (2021). Hypoxia Promotes Pancreatic Cancer Cell Dedifferentiation to Stem-Like Cell Phenotypes With High Tumorigenic Potential by the HIF-1α/Notch Signaling Pathway. Pancreas *50*, 756–765.
38. Huang, S.F., Yang, Z.L., Li, D.Q., Liu, Z.Y., Wang, C.W., Miao, X.Y., Zou, Q., and Yuan, Y. (2016). Jagged1 and DLL4 expressions in benign and malignant pancreatic

lesions and their clinicopathological significance. Hepatobiliary Pancreat. Dis. Int. *15*, 640–646.

39. Tang, Z., Li, C., Kang, B., Gao, G., Li, C., and Zhang, Z. (2017). GEPIA: a web server for cancer and normal gene expression profiling and interactive analyses. Nucleic Acids Res. *45* (W1), W98–W102.

40. Nagy, Á., Lánczky, A., Menyhárt, O., and Győrffy, B. (2018). Validation of miRNA prognostic power in hepatocellular carcinoma using expression data of independent datasets. Sci. Rep. *8*, 9227.

41. Vasaikar, S.V., Straub, P., Wang, J., and Zhang, B. (2018). LinkedOmics: analyzing multi-omics data within and across 32 cancer types. Nucleic Acids Res. *46* (D1), D956–D963.

42. Rhodes, D.R., Yu, J., Shanker, K., Deshpande, N., Varambally, R., Ghosh, D., Barrette, T., Pandey, A., and Chinnaiyan, A.M. (2004). ONCOMINE: a cancer microarray database and integrated data-mining platform. Neoplasia *6*, 1–6.

43. Zhang, R., Liu, Q., Peng, J., Wang, M., Gao, X., Liao, Q., and Zhao, Y. (2019). Pancreatic cancer-educated macrophages protect cancer cells from complement-dependent cytotoxicity by up-regulation of CD59. Cell Death Dis. *10*, 836.

44. Liu, Q., Wu, H., Li, Y., Zhang, R., Kleeff, J., Zhang, X., Cui, M., Liu, J., Li, T., Gao, J., et al. (2020). Combined blockade of TGf-β1 and GM-CSF improves chemotherapeutic effects for pancreatic cancer by modulating tumor microenvironment. Cancer Immunol. Immunother. *69*, 1477–1492.

45. Liu, Q., Li, Y., Niu, Z., Zong, Y., Wang, M., Yao, L., Lu, Z., Liao, Q., and Zhao, Y. (2016). Atorvastatin (Lipitor) attenuates the effects of aspirin on pancreatic cancerogenesis and the chemotherapeutic efficacy of gemcitabine on pancreatic cancer by promoting M2 polarized tumor associated macrophages. J. Exp. Clin. Cancer Res. *35*, 33.

46. Liu, Q., Zhang, R., Zhang, X., Liu, J., Wu, H., Li, Y., Cui, M., Li, T., Song, H., Gao, J., et al. (2021). Dopamine improves chemotherapeutic efficacy for pancreatic cancer by regulating macrophage-derived inflammations. Cancer Immunol. Immunother. *70*, 2165–2177.

47. Shen, J., Cao, B., Wang, Y., Ma, C., Zeng, Z., Liu, L., Li, X., Tao, D., Gong, J., and Xie, D. (2018). Hippo component YAP promotes focal adhesion and tumour aggressiveness via transcriptionally activating THBS1/FAK signalling in breast cancer. J. Exp. Clin. Cancer Res. *37*, 175.